Direct synthesis of doubly deprotonated, dearomatised lutidine PNP Cr and Zr pincer complexes based on isolated K and Li ligand transfer reagents

Thomas Simler, Gilles Frison, Pierre Braunstein, Andreas A. Danopoulos

Dalton Transactions

COMMUNICATION

View Article Online
View Journal | View Issue

Cite this: *Dalton Trans.*, 2016, **45**, 2800

Received 30th November 2015,
Accepted 18th January 2016

DOI: 10.1039/c6dt00144k

www.rsc.org/dalton

Direct synthesis of doubly deprotonated, dearomatised lutidine PNP Cr and Zr pincer complexes based on isolated K and Li ligand transfer reagents†

Thomas Simler,[a] Gilles Frison,[b] Pierre Braunstein*[a] and Andreas A. Danopoulos*[a,c]

Double deprotonation of 2,6-bis-(di-*tert*-butylphosphinomethyl)-pyridine (^{tBu}PN^{tBu}P), with $KCH_2C_6H_5$ afforded K_2(^{tBu}P*N$_a$^{tBu}P*), N$_a$ = anionic amido N, ^{tBu}P* = di-*tert*-butyl vinylic P donor. The analogous [Li$_2$(^{tBu}P*N$_a$^{tBu}P*)]$_2$ (1) was reacted with [CrCl$_2$(THF)$_2$] and [ZrCl$_4$(THT)$_2$] to give the helical [Cr{Cr(^{tBu}P*N$_a$^{tBu}P*)Cl}$_2$] (2) and [Zr(^{tBu}P*N$_a$^{tBu}P*)Cl$_2$] (3), respectively. DFT calculations support dearomatisation of P*N$_a$P* and its high donor ability.

'Pincer' ligands attract continuing interest due to the formation of stable, well-defined and finely-tunable complexes.[1] From the large diversity currently available, designs bearing diphosphines attached to the monoanionic *m*-(α,α′)-xylylenyl-, (^{R}PC^{R}P), and the neutral 2,6-lutidine-backbones (^{R}PN^{R}P),[2] R = carbon substituent at P (Scheme 1), have found wider application in catalysis, materials and biomedicine, in particular with late transition metals.[3] In comparison, examples of ^{R}PN^{R}P ligands coordinated to early and/or electropositive metals are rare (*e.g.* Cr,[4] Mo[5] and W[6]). Catalytic applications with 3d-transition metal ^{R}PN^{R}P complexes have also emerged.[4,7] Recent reaction mechanisms for the activation of small molecules by ^{R}PN^{R}P complexes involve as key catalytic steps protonation-monodeprotonation at one α-methylene arm, accompanied by aromatisation–dearomatisation of the lutidine ring, in support of metal–ligand cooperation in ^{R}PN$_a$^{R}P* (N$_a$ = anionic amido N donor, P* = vinylic P donor)[8] systems.[3c,9]

However, reports on complexes with two mono-deprotonated α-methylene arms of PCP and PNP skeletons are scarce,[10] probably due to the high reactivity of the resulting products and the lack of general synthetic access. To the best of our knowledge, there is only one report of structurally characterised ^{R}P*N$_a$^{R}P* complexes, obtained from coordinated PNP on a Ni^{II} centre.[10d] Occasionally 'sluggish' (using KN(SiMe$_3$)$_2$) or requiring large excess of base (with MeLi),[10c] and lacking generality,[10e] abstractions of *both* the α- and α′-C*H*$_2$^{R}P of coordinated ^{R}PN^{R}P (leading to dianionic ^{R}P*N$_a$^{R}P*) have resulted in Pd^{II}, Pt^{II},[10c,f] and recently Re^{IV} (R = ^{t}Bu) complexes,[10e] which were characterised only *in situ* by NMR techniques. Relevant deprotonation at both –N*H*– linkers of a cobalt bis(aminophosphine) PNP analogue has been postulated in the generation of catalytic species.[11]

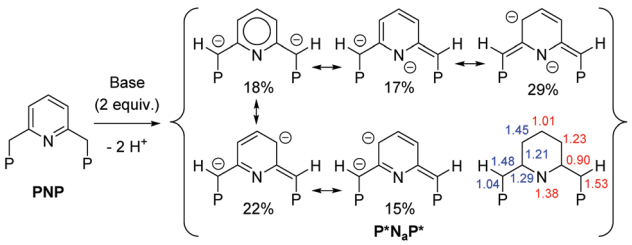

Scheme 1 Double deprotonation of ^{R}PN^{R}P and relevant resonance structures of ^{R}P*N$_a$^{R}P*. NBO weight of the resonance structures, electronic π-populations (in red) and Wiberg bond indexes (in blue) calculated for R = Me at the M06-2X/6-31++G(d,p) level of theory.

While ^{R}PN$_a$^{R}P* complexes are usually accessed by deprotonation with bulky external amide bases (pK_a ≈ 26–37 in THF)[12] of one α-C*H*$_2$^{R}P in preformed P^{R}N^{R}P complexes, this method has limited applicability to the deprotonation of *both* the α- and α′-C*H*$_2$^{R}P. Alternatively, organolithium bases (pK_a ≈ 40–56)[13] have been used for the *in situ* formation of ^{R}P*C^{R}P*–Pt^{II} and ^{R}P*N$_a$^{R}P*–Rh^{I} complexes (R = Ph), that were further quenched with electrophiles (*vide supra*).[10a,b] Stronger, more aggressive bases may lead to undesirable side reactions, limiting the scope of the approach. In contrast, transfer reagents (*e.g.* based on alkali metals) allowing direct complexation of ^{R}P*N$_a$^{R}P* have not been reported and may overcome the aforementioned synthetic difficulties.

[a]*Laboratoire de Chimie de Coordination, Institut de Chimie (UMR 7177 CNRS), Université de Strasbourg, 4 rue Blaise Pascal, 67081 Strasbourg, France*
[b]*LCM, CNRS, Ecole polytechnique, Université Paris-Saclay, 91128 Palaiseau, France*
[c]*Institute for Advanced Study (USIAS), Université de Strasbourg, France.*
E-mail: braunstein@unistra.fr, danopoulos@unistra.fr

†Electronic supplementary information (ESI) available: Experimental procedures, spectroscopic data, X-ray data and computational details. CCDC 1427661–1427663. For ESI and crystallographic data in CIF or other electronic format see DOI: 10.1039/c6dt00144k

Herein, we disclose K and Li complexes of $^{R}P^{*}N_{a}{}^{R}P^{*}$, as new reagents that allow the preparation of unprecedented metal complexes. The structural diversity of the latter illustrates the versatility of $^{R}P^{*}N_{a}{}^{R}P^{*}$ arising from its extended electronic delocalisation, also studied by DFT methods (Scheme 1).

Complete conversion of $^{t\mathrm{Bu}}PN^{t\mathrm{Bu}}P$ to the doubly deprotonated $^{t\mathrm{Bu}}P^{*}N_{a}{}^{t\mathrm{Bu}}P^{*}$ succeeded with the potent benzyl potassium (KBn, pK_a = *ca.* 42 in polar aprotic solvents).[14] Thus, monitoring by ^{1}H-NMR the reaction of 2 equiv. KBn with a THF or toluene solution of $^{t\mathrm{Bu}}PN^{t\mathrm{Bu}}P$ at −78 °C revealed the formation of a new species (δ 6.38 (1H), 4.99 (2H) and 3.00 (2H) in C_6D_6); in addition, a broad $^{31}P\{^{1}H\}$-NMR singlet at δ 13.1 (*cf.* δ 35.2 for $^{t\mathrm{Bu}}PN^{t\mathrm{Bu}}P$) was observed, all these data being consistent with a symmetrical species in solution (for more details see section I.3.1 in ESI†). It was tentatively assigned to the symmetrical dianion $^{t\mathrm{Bu}}P^{*}N_{a}{}^{t\mathrm{Bu}}P^{*}$ (Scheme 1). Although single crystals suitable for X-ray diffraction could not be obtained, evidence for the double deprotonation was obtained by the reaction with D_2O and the resulting isotopomer α,α′-d_2-$^{t\mathrm{Bu}}PN^{t\mathrm{Bu}}P$ was characterised by NMR spectroscopy (section I.4 in ESI†). Moreover, a NOESY experiment in THF established the presence of an equilibrium between different geometric isomers of $K_2(^{t\mathrm{Bu}}P^{*}N_{a}{}^{t\mathrm{Bu}}P^{*})$ due to rotation about the PC···C bonds (see section I.3.2 in ESI†).

More detailed characterisation of the dianion $^{t\mathrm{Bu}}P^{*}N_{a}{}^{t\mathrm{Bu}}P^{*}$ succeeded by using organolithium bases. Thus, reaction of two equiv. $LiCH_2SiMe_3$ with $^{t\mathrm{Bu}}PN^{t\mathrm{Bu}}P$ in C_6D_6 led to the slow formation of $[Li_2(^{t\mathrm{Bu}}P^{*}N_{a}{}^{t\mathrm{Bu}}P^{*})]_2$ (**1**) with NMR data supporting the presence of a symmetrical doubly deprotonated species. A more useful protocol to access $[Li_2(^{t\mathrm{Bu}}P^{*}N_{a}{}^{t\mathrm{Bu}}P^{*})]_2$ was developed by using ^{t}BuLi.[15] The reaction proceeded fast at r.t. in pentane, from which **1** conveniently precipitated and was isolated by filtration as a yellow, extremely air-sensitive solid (up to 2 g scale, 75%). Evidence for the double deprotonation was again obtained by the reaction of **1** with D_2O (section I.4 in ESI†). The structure of **1** was determined from a yellow crystal formed during the reaction of a C_6D_6 solution of $^{t\mathrm{Bu}}PN^{t\mathrm{Bu}}P$ with excess $LiCH_2SiMe_3$ (see above). The structure reveals a centrosymmetric dimeric aggregate with the two heterocyclic rings being 4.090 Å apart (Fig. 1). In each constitutive planar subunit, one Li atom is in a T-shaped environment (two P* and the N_a) (P–Li–P = 167.6°). Two additional Li atoms bridge these two subunits through two η^3-allylic-type interactions involving the $CH_{\alpha\text{-}P}$, $C_{\alpha\text{-}N}$ and $C_{\beta\text{-}N}$ atoms of the heterocycle (crystallographic C6–C1–C2 and C15–C5–C4). A relevant η^3-allylic interaction with Li^+ has been described in the ion pair $[Li(ether)_2][Ni^{II}(^{t\mathrm{Bu}}P^{*}N_{a}{}^{t\mathrm{Bu}}P^{*})Me]$.[10d] It is plausible that the P-atom adjacent to the deprotonated site in the 2,6-lutidine backbone contributes to the stabilisation of the dianion in **1**.[16] DFT calculations on the model ligands $^{Me}PN^{Me}P$, $^{Me}PN_{a}{}^{Me}P^{*}$ (for comparison) and $^{Me}P^{*}N_{a}{}^{Me}P^{*}$ shed light on their electronic structures. They show extensive delocalisation of the 6, 8 and 10 π-electrons, respectively, as illustrated (see ESI†) by the delocalised molecular orbitals, the CC and CN bond distances that are intermediate between a single (1.54 and 1.47 Å) and a double bond (1.34 and 1.29 Å), respectively, as well as the Wiberg bond indexes for the CC and CN bonds, which range from 1.21 to 1.48 for $^{Me}P^{*}N_{a}{}^{Me}P^{*}$ (Scheme 1). Delocalisation is also reflected by the number and nature of significant resonance structures, determined by the natural resonance theory (NRT),[17] which show that the anionic sites are delocalised over N, $C_{\beta\text{-}N}$ and $C_{\alpha\text{-}P}$ (Scheme 1 and ESI†). The six-membered ring of $^{Me}P^{*}N_{a}{}^{Me}P^{*}$ is populated by 6.65 π-electrons, indicating a charge transfer of *ca.* 0.3 e from each $C_{\alpha\text{-}P}$ deprotonated site. Its smaller value compared to the charge transfer from $C_{\alpha\text{-}P}$ in $^{Me}PN_{a}{}^{Me}P^{*}$ (0.5 e) is presumably due to competition between the two anionic sites.

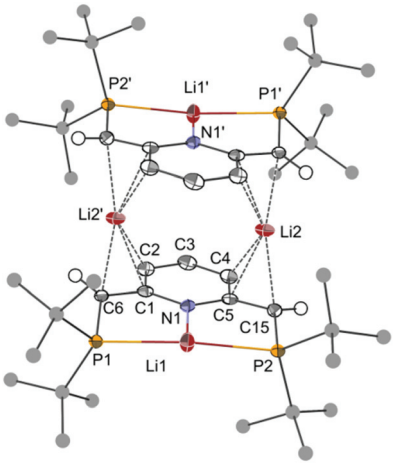

Fig. 1 The centrosymmetric structure of **1** with ellipsoids at 40% probability except the ^{t}Bu atoms that are depicted as spheres. H atoms are omitted except for the α-CHP.

Consequently, the π-population at $C_{\alpha\text{-}P}$ is higher in $^{Me}P^{*}N_{a}{}^{Me}P^{*}$ than in $^{Me}PN_{a}{}^{Me}P^{*}$ (1.53 e *vs.* 1.42 e), which also induces larger stabilisation of the anionic site by hyperconjugation with the σ* P–C_{Me} bond, as revealed by the shorter P–C bond length (1.774 *vs.* 1.790 Å) and the larger lone pair → σ* second-order interaction energy (95 *vs.* 73 kJ mol^{-1}) (from NBO analysis). Lastly, as for $^{Me}PN_{a}{}^{Me}P^{*}$ (NICS(0) value: +1.6), $^{Me}P^{*}N_{a}{}^{Me}P^{*}$ shows dearomatisation of the pyridine ring (NICS(0) value: +1.0) relative to the neutral $^{Me}PN^{Me}P$ (NICS(0) value: −6.2).

The utility and potential of **1** as transmetallation reagent was demonstrated by the synthesis of Cr^{II} and Zr^{IV} complexes. Yellow **1** reacted with $[CrCl_2(THF)_2]$ at low temperatures to give the trinuclear complex $[Cr\{Cr(^{t\mathrm{Bu}}P^{*}N_{a}{}^{t\mathrm{Bu}}P^{*})Cl\}_2]$ (**2**), isolated as red air sensitive crystals from pentane (Scheme 2).

This unusual complex is paramagnetic, with μ_{eff} = 8.50μ_B (Evans' method in THF, see ESI†), a value consistent with three uncoupled Cr(II) (d^4, S = 2) centres giving rise to a spin-only moment of 8.48μ_B. The trinuclear structure of **2** (Fig. 2) features two terminal subunits, each comprising one 12 electron Cr centre coordinated to a (κP,κN_a,κP) donor set in a distorted square planar environment completed by a Cl ligand, and one internal 12 electron Cr linking the two subunits *via* two η^3-allylic-type interactions, through their $CH_{\alpha\text{-}P}$, $C_{\alpha\text{-}N}$ and

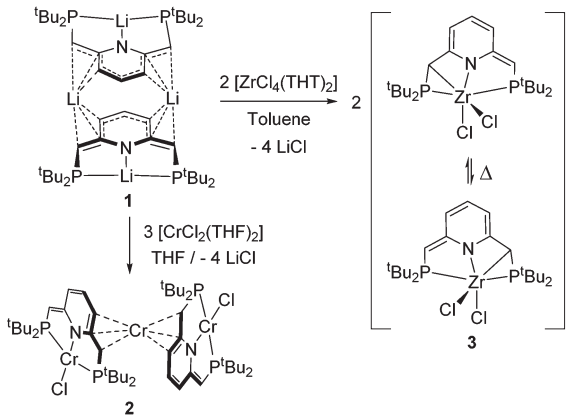

Scheme 2 Synthesis of [Cr{Cr($^{t\mathrm{Bu}}$P*N$_a$$^{t\mathrm{Bu}}$P*)Cl}$_2$] (**2**) and [Zr($^{t\mathrm{Bu}}$P*-N$_a$$^{t\mathrm{Bu}}$P*)Cl$_2$] (**3**) by transmetallation from **1**.

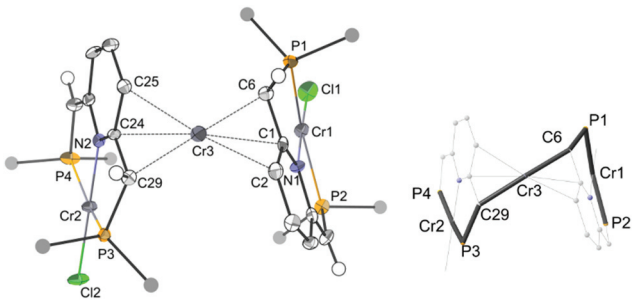

Fig. 2 The structure of [Cr{Cr($^{t\mathrm{Bu}}$P*N$_a$$^{t\mathrm{Bu}}$P*)Cl}$_2$] (**2**) with ellipsoids at 30% probability (left). Only one ^{t}Bu carbon is shown as a sphere and H-atoms are omitted, except for the α-C*H*. Stick representation of the helical chirality (right).

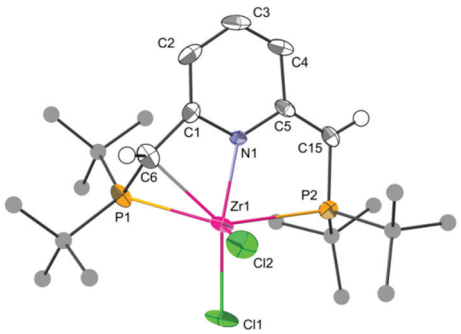

Fig. 3 The molecular structure of one of the two [Zr($^{t\mathrm{Bu}}$P*N$_a$$^{t\mathrm{Bu}}$P*)Cl$_2$] (**3**) units with ellipsoids at 30% except the ^{t}Bu atoms that are depicted as spheres. H-atoms are omitted, except for the α-C*HP* (see ESI† for the second independent molecule of **3**).

$C_{\beta\text{-}N}$ backbone atoms. The overall approximate molecular symmetry of helical **2** is C_2 (chiral space group $P2_12_12_1$, Flack parameter = 0.002(18)). The allylic moieties are in an 'eclipsed-like' arrangement whereas in the known [Cr(allyl)$_2$] (allyl = bulky 1,3-bis(trimethylsilyl)allyl), the molecular symmetry is C_{2h} and the conformation 'staggered'.[18] The Cr–N bond lengths (2.052(6) and 2.058(6) Å) are in the high range of anionic Cr–N$_a$ [19] but shorter than the Cr–N$_{pyridine}$ in [Cr(^{Ph}PN^{Ph}P)Cl$_2$] (2.164(2) Å).[4] The C–C distances within the allylic units are unequal (1.408(10), 1.442(10) Å and 1.389(10), 1.449(10) Å, respectively) and the six Cr–C$_{allyl}$ bonds show also substantial variation (2.175(8)–2.393(8) Å).

No intermediate was isolated in the formation of **2**, but it is reasonable to assume that the two pincer units are initially formed leading to '*ate*' type Cr–Li complexes, or ion pairs *e.g.* [Li(THF)$_x$][Cr^{II}($^{t\mathrm{Bu}}$P*N$_a$$^{t\mathrm{Bu}}$P*)Cl],[10d] that subsequently react with [CrCl$_2$(THF)$_2$] to form **2**. Alternative bonding modes of the $^{t\mathrm{Bu}}$P*N$_a$$^{t\mathrm{Bu}}$P*, in particular on a single (electropositive, d^0, large size) metal ion are conceivable, and shown with [Zr($^{t\mathrm{Bu}}$P*N$_a$$^{t\mathrm{Bu}}$P*)Cl$_2$] (**3**), obtained as dark-green crystals by reaction of **1** with [ZrCl$_4$(THT)$_2$], THT = tetrahydrothiophene, in toluene at −78 °C (Scheme 2). Its structure (Fig. 3) reveals an unexpected coordination mode of the $^{t\mathrm{Bu}}$P*N$_a$$^{t\mathrm{Bu}}$P* ligand, featuring anionic phosphinoalkanide functionality (*cf.* phosphino-methanides),[20] tethered to the anionic heterocycle. Comparison of the metrical data in **3** (short Zr–P and Zr–C$_{\alpha\text{-}P}$ bonds) supports an η^2-(P–C) coordination (up to 10 e$^-$ donor, dianionic ligand). Overall, the coordination geometry at Zr can be described as distorted octahedral. Interestingly, the ligand departs from planarity (*cf.* **2**) and the heterocyclic ring remains dearomatised. The Zr–P bond distances are different (2.643(2) Å and 2.811(2) Å) and the Zr–N bond distance (2.120(4) Å) is typical for a Zr–N$_{amido}$ bond (mean Zr–N$_{amido}$ 2.12(9) Å).[19]

The unsymmetrical arrangement seen in the solid state is retained in C_6D_6 solution at room temperature: in the ^{31}P{^{1}H}-NMR spectrum two closely spaced, broad singlets can be assigned to the inequivalent P arms (at δ 56.0 and 55.2); the appearance of the spectrum is field-independent, and upon heating to 70 °C, it coalesced to one singlet at δ 56.5, indicating non-rigidity. In pentane, two broad singlets were observed also at r.t., which upon cooling to −40 °C split into two weakly coupled doublets. The ^{1}H-NMR data are consistent with an oscillation of the Zr centre within the ligand pocket (section I.6 in ESI† and Scheme 2) ($\Delta G^{\neq}$ = 62 ± 2 kJ mol^{-1}). This assumption has been confirmed by DFT calculations which allow locating a symmetric transition state situated 63 kJ mol^{-1} above [Zr(^{Me}P*N$_a$^{Me}P*)Cl$_2$] (**3′**, as model for **3**). Furthermore, an energy decomposition analysis combined with the natural orbitals for chemical valence scheme (ETS-NOCV)[21] was conducted on **3′**. The total ^{Me}P*N^{Me}P*–ZrCl$_2$ interaction energy is estimated at −2801 kJ mol^{-1}. Due to the dicationic and dianionic nature of the interacting fragments, electrostatic interactions contribute significantly (−2270 kJ mol^{-1}, *i.e.* 61%) to the attractive interactions, the remaining 39% (−1462 kJ mol^{-1}) being due to covalent bonding, whereas the Pauli repulsion term amounts to 931 kJ mol^{-1}. The orbital interactions can be further decomposed into contributions related to the deformation density due to the bonding. Fig. 4 shows the deformation densities corresponding to the five most important orbital interactions as well as their calculated strength Δ*E*.

The deformation densities in Fig. 4a and e illustrate the σ-donation of the out-of-phase and in-phase combinations of

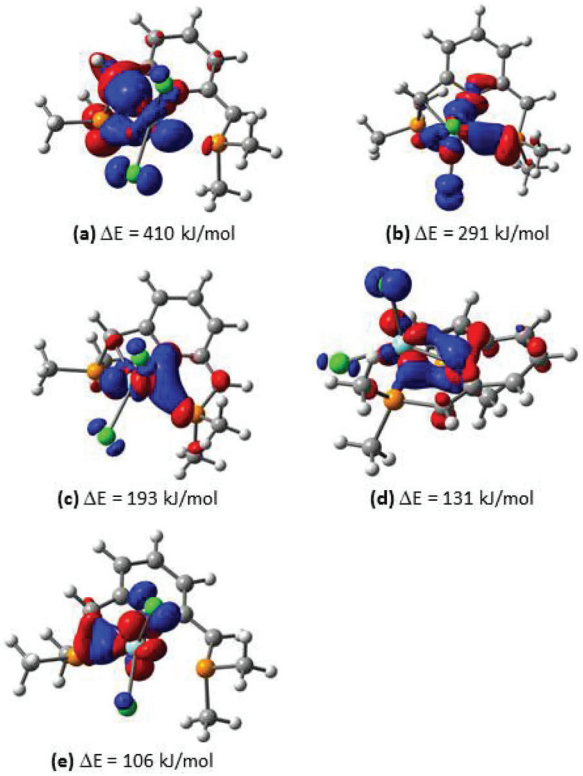

Fig. 4 Deformation densities associated with the orbital interactions in [Zr(^{Me}P*N$_a$^{Me}P*)Cl$_2$]. The charge flow of the electronic density is red → blue.

the two lone pairs at P1 and C6 (Fig. 3) to the metal, the former being the dominant term of the orbital interaction. Similar σ-donation type deformation densities are observed from the two σ lone pairs at N1 and P2 (Fig. 4b and c). The deformation density in Fig. 4d displays the weak charge flow that originates from the π-interaction between the six-membered ring and the metal. This decomposition confirms the very high donor ability of P*N$_a$P*.

In conclusion, the choice of strong bases and conditions has allowed the first isolation of the pure K and Li salts of the dearomatised, doubly deprotonated ^{tBu}P*N$_a$^{tBu}P* ligand and [Li$_2$(^{tBu}P*N$_a$^{tBu}P*)]$_2$ was structurally characterised. They provide a new and efficient route to access doubly deprotonated and dearomatised transition metal complexes with unprecedented structures by transmetallation reactions, as illustrated with Cr^{II} and Zr^{IV}. This versatile procedure extends the scope of the ^{R}P*N$_a$^{R}P* ligand to early transition metal centres. Considering the high and increasing importance of (doubly) deprotonated and dearomatised pincer complexes in catalysis, such systems are good candidates for metal–ligand cooperativity.[9c]

The USIAS, CNRS, Unistra, Région Alsace and Communauté Urbaine de Strasbourg are acknowledged for the award of fellowships and a Gutenberg Excellence Chair (2010-11) to AAD. We thank the CNRS and the MESR (Paris) for funding and for a PhD grant to TS. We are grateful to Dr L. Karmazin (Service de Radiocristallographie, Unistra) for solving the crystal structures and Dr B. Vincent (Service de Résonance Magnétique Nucléaire, Unistra) for the VT analysis. Calculations were performed using HPC resources from GENCI-IDRIS (Grant 2015-086894). GF thanks C. Clavaguéra for technical support for the NRT calculations.

References

1 (*a*) *The Chemistry of Pincer Compounds*, ed. D. Morales-Morales and C. M. Jensen, Elsevier Science B.V., Amsterdam, The Netherlands, 2007; (*b*) *Organometallic Pincer Chemistry*, ed. G. van Koten and D. Milstein, Springer, Berlin Heidelberg, 2013; (*c*) *Pincer and Pincer-Type Complexes: Applications in Organic Synthesis and Catalysis*, ed. K. J. Szabó and O. F. Wendt, Wiley-VCH, Weinheim, Germany, 2014.

2 (*a*) M. Kawatsura and J. F. Hartwig, *Organometallics*, 2001, **20**, 1960; (*b*) D. Hermann, M. Gandelman, H. Rozenberg, L. J. W. Shimon and D. Milstein, *Organometallics*, 2002, **21**, 812.

3 (*a*) J. Choi, A. H. R. MacArthur, M. Brookhart and A. S. Goldman, *Chem. Rev.*, 2011, **111**, 1761; (*b*) N. Selander and K. J. Szabó, *Chem. Rev.*, 2011, **111**, 2048; (*c*) C. Gunanathan and D. Milstein, *Chem. Rev.*, 2014, **114**, 12024.

4 A. Alzamly, S. Gambarotta and I. Korobkov, *Organometallics*, 2013, **32**, 7204.

5 (*a*) H.-F. Lang, P. E. Fanwick and R. A. Walton, *Inorg. Chim. Acta*, 2002, **329**, 1; (*b*) K. Arashiba, Y. Miyake and Y. Nishibayashi, *Nat. Chem.*, 2011, **3**, 120.

6 K. Arashiba, K. Sasaki, S. Kuriyama, Y. Miyake, H. Nakanishi and Y. Nishibayashi, *Organometallics*, 2012, **31**, 2035.

7 (*a*) J. I. van der Vlugt, *Eur. J. Inorg. Chem.*, 2012, 363; (*b*) J. V. Obligacion, S. P. Semproni and P. J. Chirik, *J. Am. Chem. Soc.*, 2014, **136**, 4133; (*c*) M. L. Scheuermann, S. P. Semproni, I. Pappas and P. J. Chirik, *Inorg. Chem.*, 2014, **53**, 9463; (*d*) T. Zell and D. Milstein, *Acc. Chem. Res.*, 2015, **48**, 1979.

8 The notations ^{R}PN$_a$^{R}P* and ^{R}P*N$_a$^{R}P* designate structures corresponding to resonance forms where the anionic charge in on N (see Scheme 1).

9 (*a*) J. I. van der Vlugt and J. N. H. Reek, *Angew. Chem., Int. Ed.*, 2009, **48**, 8832; (*b*) R. Tanaka, M. Yamashita, L. W. Chung, K. Morokuma and K. Nozaki, *Organometallics*, 2011, **30**, 6742; (*c*) J. R. Khusnutdinova and D. Milstein, *Angew. Chem., Int. Ed.*, 2015, **54**, 12236.

10 (*a*) F. Gorla, L. M. Venanzi and A. Albinati, *Organometallics*, 1994, **13**, 43; (*b*) C. Hahn, M. Spiegler, E. Herdtweck and R. Taube, *Eur. J. Inorg. Chem.*, 1998, 1425; (*c*) M. Feller, E. Ben-Ari, M. A. Iron, Y. Diskin-Posner, G. Leitus, L. J. W. Shimon, L. Konstantinovski and D. Milstein, *Inorg. Chem.*, 2010, **49**, 1615; (*d*) M. Vogt, O. Rivada-Wheelaghan, M. A. Iron, G. Leitus, Y. Diskin-Posner, L. J. W. Shimon, Y. Ben-David and D. Milstein, *Organometallics*, 2013, **32**,

300; (*e*) T. J. Korstanje, M. Lutz, J. T. B. H. Jastrzebski and R. J. M. Klein Gebbink, *Organometallics*, 2014, **33**, 2201; (*f*) W. D. Bailey, W. Kaminsky, R. A. Kemp and K. I. Goldberg, *Organometallics*, 2014, **33**, 2503.

11 S. Rösler, J. Obenauf and R. Kempe, *J. Am. Chem. Soc.*, 2015, **137**, 7998.

12 (*a*) R. R. Fraser, T. S. Mansour and S. Savard, *J. Org. Chem.*, 1985, **50**, 3232; (*b*) R. R. Fraser, M. Bresse and T. S. Mansour, *J. Chem. Soc., Chem. Commun.*, 1983, 620.

13 (*a*) F. G. Bordwell, *Acc. Chem. Res.*, 1988, **21**, 456; (*b*) M. Stratakis, P. G. Wang and A. Streitwieser, *J. Org. Chem.*, 1996, **61**, 3145.

14 F. G. Bordwell, D. Algrim and N. R. Vanier, *J. Org. Chem.*, 1977, **42**, 1817.

15 H. J. Reich, *Chem. Rev.*, 2013, **113**, 7130.

16 (*a*) K. Izod, *Coord. Chem. Rev.*, 2002, **227**, 153; (*b*) T. Leyssens and D. Peeters, *J. Org. Chem.*, 2008, **73**, 2725.

17 E. D. Glendening and F. Weinhold, *J. Comput. Chem.*, 1998, **19**, 593.

18 J. D. Smith, T. P. Hanusa and V. G. Young, *J. Am. Chem. Soc.*, 2001, **123**, 6455.

19 The Cambridge Structural Database, accessed Jan. 2016: F. Allen, *Acta Crystallogr., Sect. B: Struct. Sci.*, 2002, **58**, 380.

20 (*a*) S. J. Young, M. M. Olmstead, M. J. Knudsen and N. E. Schore, *Organometallics*, 1985, **4**, 1432; (*b*) H. H. Karsch, B. Deubelly, J. Hofmann, U. Pieper and G. Mueller, *J. Am. Chem. Soc.*, 1988, **110**, 3654.

21 M. P. Mitoraj, A. Michalak and T. Ziegler, *J. Chem. Theory Comput.*, 2009, **5**, 962.

